PAUL SCHERRER INSTITUT PSI

FONDAZIONE BRUNO KESSLER

Antonio Liguori – Università di Bari “Aldo Moro” – Trainee at PSI PS Detector Group

Investigation of soft X-ray detection with iLGAD sensors

01.03.2023 – 18th Trento Workshop on Advanced Silicon Radiation Detectors

Email: antonio.liguori@psi.ch

Introduction

Soft X-ray applications at Synchrotrons and FELs (250 eV – 2 keV)

- Access K-edges of biologically relevant elements e.g. in water window 250-520 eV
- L-edges of 3d transition metals, Fe, Cu, etc.

Possible applications:

- Proteins and Pharmaceutical
- Magnetic domains
- Quantum materials
- Bio-imaging.

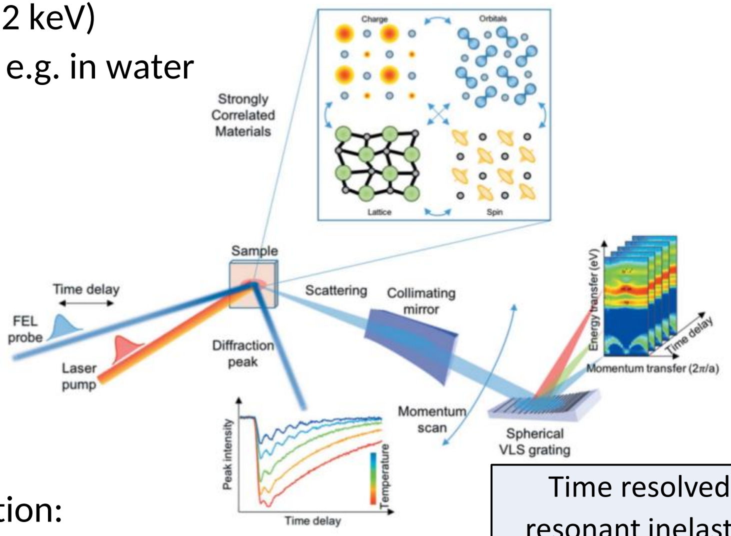

Time resolved resonant inelastic X-ray scattering

Current **limitations of hybrid detectors** for soft X-ray detection:

- **Low quantum efficiency** (QE);
- **Electronic noise** → low signal to noise ratio (SNR).

PSI and **FBK** collaborate for the developement of **iLGAD sensors** with **optimized entrance window** for soft X-Ray detection.

Soft X-ray detection with iLGAD

iLGAD layout:

- 100% fill factor;
- Interpolation through charge sharing for high spatial resolution;
- Hole collection;
- Double sided process;
- Needs to be compatible with optimized entrance window;
- Multiplication factor depends on depth where X-rays absorbed.

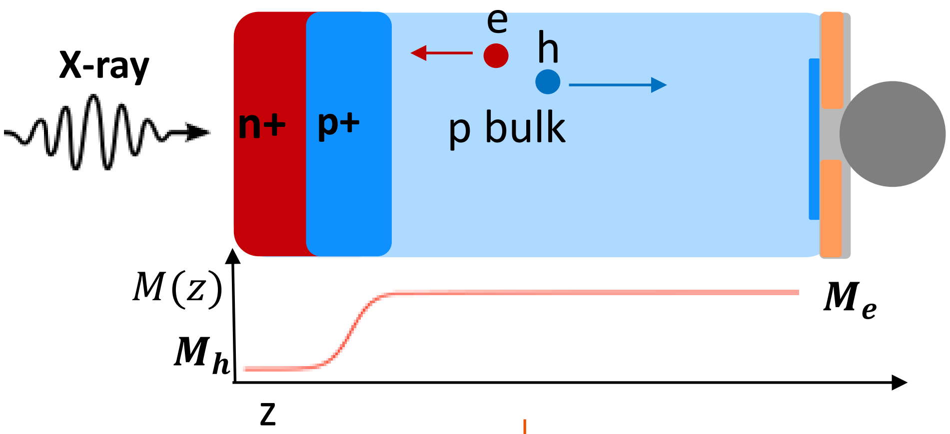

Multiplication factor $M(z)$ **increases from M_h to M_e** with absorption depth z

Test of iLGADs with optimized entrance window

- **8 iLGAD process splits from FBK**
- 275 μm thick with **different entrance window and gain layer (GL)** designs.
- Measurements at Synchrotron (**SLS**), $\boldsymbol{E_{ph} \in [200eV, 1keV]}$.

In vacuum
+20°C
300V

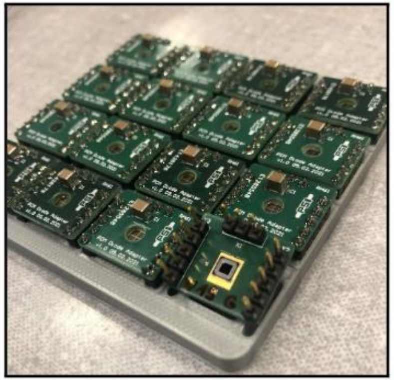

→ **p-n Diodes** → $QE(E_{ph})$

→ **iLGAD diodes**: $I_{ph}(E_{ph})$ → $gain(E_{ph})$

In vacuum
-40°C
300V

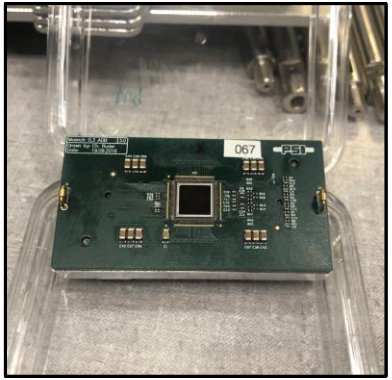

Pixelated iLGADs
(25μm pitch)
charge integrating
Mönch readout

→ **Spectra**

p-n diodes: QE vs E_{ph}

QE vs E_{ph} - UShallow n^+ (W13)

Absorption Edges of passivation

$\boldsymbol{QE(250eV)} > 60\%$

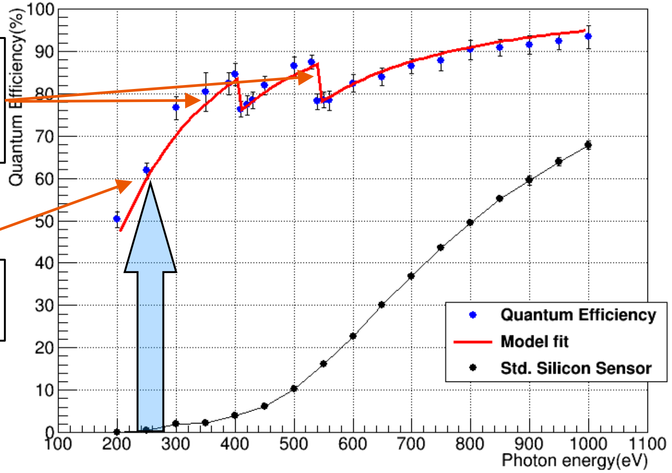

QE model:

$$QE(E_{ph}) = e^{\frac{-l_1}{\lambda_1(E_{ph})}} e^{\frac{-l_2}{\lambda_2(E_{ph})}} \int_0^W \frac{e^{\frac{-z}{\lambda_{Si}(E_{ph})}}}{\lambda_{Si}(E_{ph})} CCE(z)dz$$

From ratio at edges $\frac{\boldsymbol{QE(E^+_{edge})}}{\boldsymbol{QE(E^-_{edge})}}$ → $l_1 + l_2 \sim 85nm$

From **fit** of l_1, l_2, l_d with dead layer CCE:

$$CCE(z) = \begin{cases} 0 \ if \ z \leq l_d \\ 1 \ if \ z > l_d \end{cases}$$

→ $l_d < 1nm$

High CCE: Almost complete charge collection

iLGAD diodes: Gain vs E_{ph}

Average gain vs E_{ph}

Measured at +20°C

Linear and expon. fit: overlapping best fit function

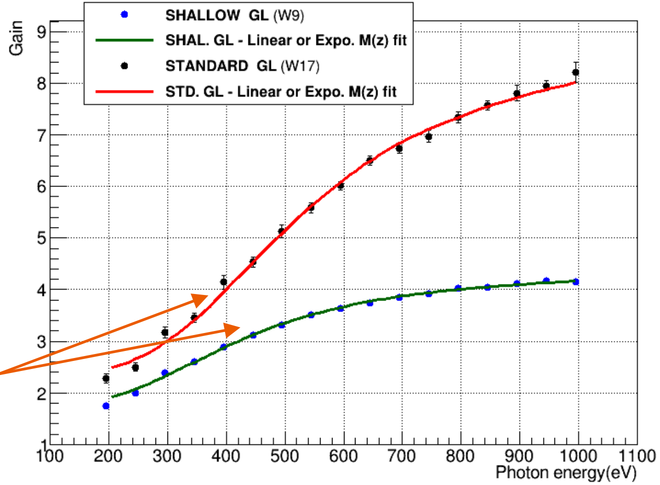

M(z)

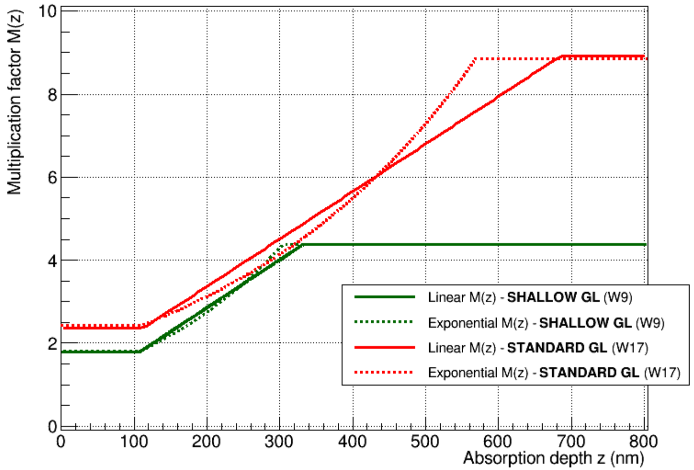

Gain expression (assuming CCE =1) :

$$g_{iLGAD}(E_{ph}) \sim \int_0^W \frac{e^{\frac{-z}{\lambda_{Si}(E_{ph})}}}{\lambda_{Si}(E_{ph})} M(z)dz$$

M(z) is extracted from the gain fit.
Linear and **exponential models used with fit parameters M_e, M_h, t_2**
t_1 is fixed from process simulation

iLGAD spectra

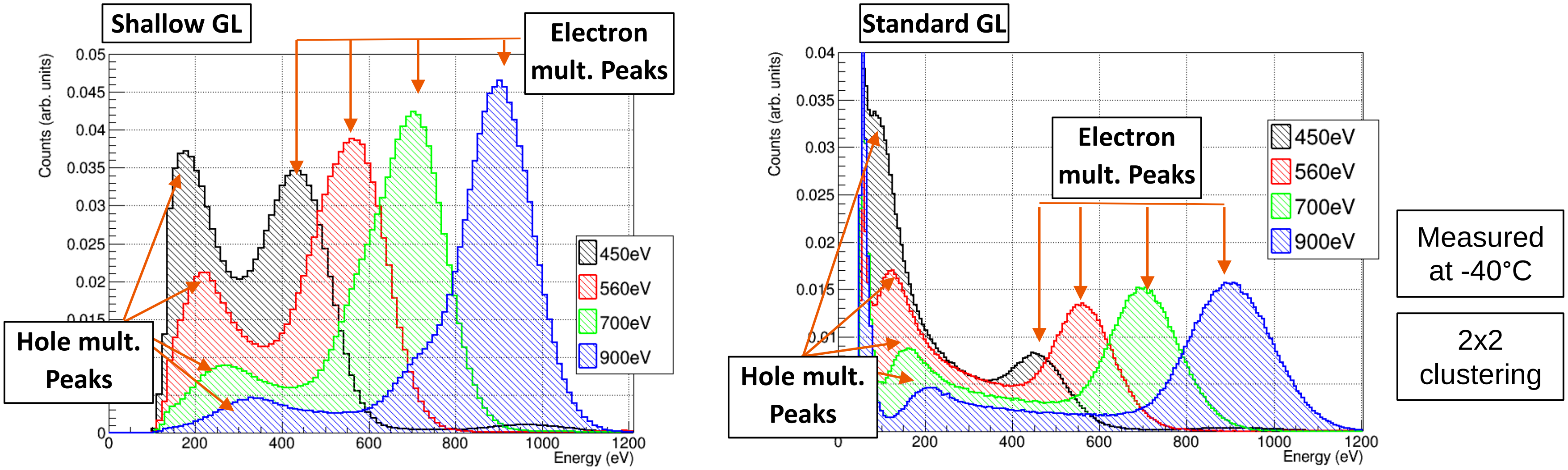

Double peaks feature due to electron and hole multiplication observed for mono-energetic soft X-rays:

- Both **peaks visible down to 450eV**.
- **Ratio of the area under peaks changes** with Eph.
- The **ratio M_h/M_e is larger for shallow GL**

} → **Depending on the gain layer design**

iLGAD spectrum simulation

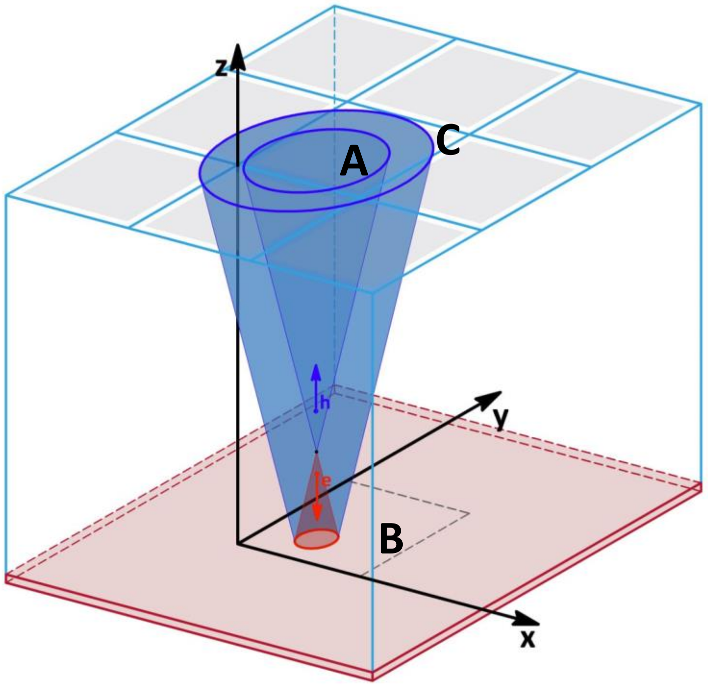

Simulation inputs:

1) Doping profiles from process simulation → E-field
2) M(z) - from gain fit + Okuto scaling of M_h and M_e
3) Detector electronic noise σ_0 - Measured

Monte Carlo Simulation:

1) Carriers generation by X-Ray absorption
2) Multiplication
3) Drift and diffusion of carriers clouds (A,B,C)

Clustering and noise:

1) 2x2 pixel clusters considered
2) Noise: gaussian fluctuations of the cluster charge with $\sigma_{noise} = 2\sqrt{\sigma_0{}^2 + \sigma_1{}^2 M(z)^2 F(z)}$

* M^2F from G.F. Dalla Betta et al. NIM A (2015)

Comparison simulated/measured spectrum

Shallow GL – Linear M(z) sim. - $E_{ph} = 500eV$

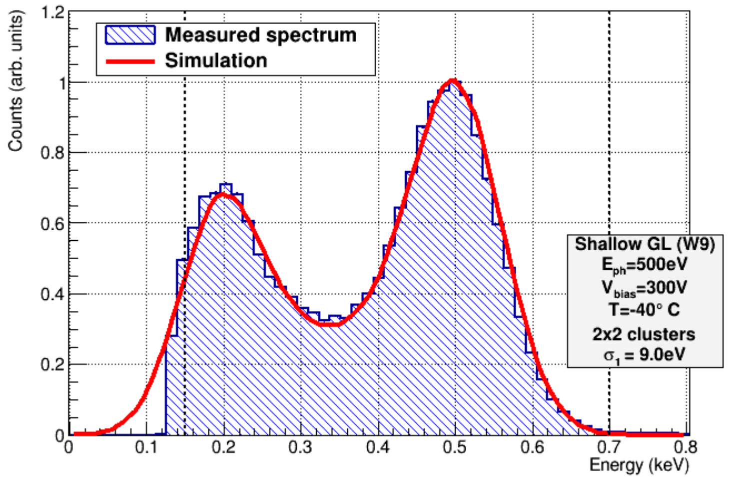

Shallow GL – Expon. M(z) sim. - $E_{ph} = 500eV$

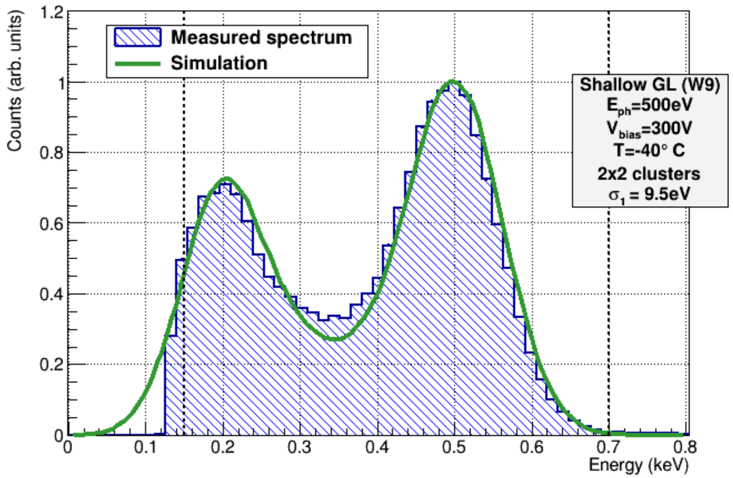

Observations:

1) Double peak feature reproduced in the simulation;
2) Okuto model provides correct scaling of ratio M_h/M_e for T change +20°C→ -40°C.
3) The shape of the valley sensitive to transition of $M(z)$ from M_h to M_e .

Linear M(z) gives better description of the measured spectrum.

Summary

Conclusions:

1) **QE** of tested wafers $> 60\%$ for photon energies $> 250eV$
2) High CCE and low noise enable the detection of **''hole-multiplication peak'' in the spectra down to 450eV**
3) **Simulations reproduce the double peak** feature of the spectrum

Next steps:

1) Simulation of the spectrum at other photon energies
2) Implementation of the simulation for different process splits
3) Studies of impact ionization in different E-field and temperature are needed for reliable predictions of iLGAD spectra with device simulation

Outlook for future developements

1) Further reduction of passivation thicknesses would improve QE
2) 2x gain increase in shallow design is needed to observe 400eV photons with $SNR > 5$ for both holes and electron multiplication peaks;
3) Shallower gain layer would enhnance probability of electron-initiated multiplication.

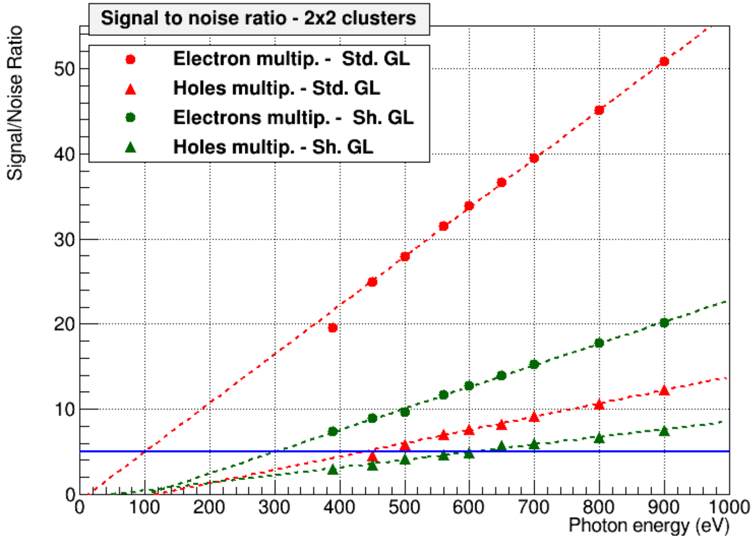

Ackowledgment

FONDAZIONE BRUNO KESSLER

Matteo Centis Vignali
Francesco Ficorella
Giacomo Borghi
Giovanni Paternoster
Maurizio Boscardin
Sabina Ronchin
Omar Hammad Ali

The Photon Science Detector Group at PSI

Back: Jiaguo Zhang, Aldo Mozzanica, Thomas King, Davide Mezza, Anna Bergamaschi, Julian B. D. Heymes. Middle: Erik Frojdh, Carlos Lopez, Martin Bruckner, Christian P. Ruder, Bernd Schmitt, Konstantinos Moustakas, Dominic Greiffenberg. Front: Viktoria Hinger, Dhanya Thattil, Roberto Dinapoli, Shqipe Hasanaj, Maria Carulla, Simon Ebner. Missing: Rebecca Barten, Pawel Kozlowski, Filippo Baruffaldi, Xiangyu Xie, Kirsty Anne Paton.

Backup slides

Attenuation length for soft X-rays

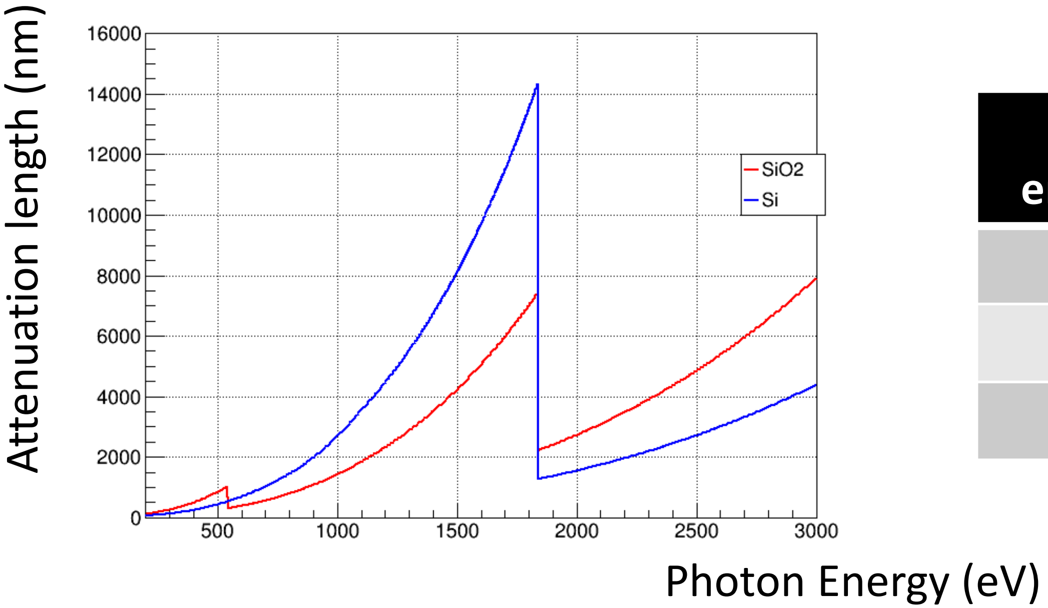

Photon energy (eV)	Att. Length in Si (microns)
251.200	9.37E-02
500.800	0.432091
800.000	1.43566

Diodes measurement setup

- Surface Interfaces Microscopy (SIM) beamline at SLS
- 3 DUT are connected to the readout board, and biased at 300V.
- The readout board is mounted on a stage together with a calibrated photodiode.

- At each energy the dark current and the current under illumination are measured for all devices.
- Temperature stabilized at +20°C with a chiller (not shown)

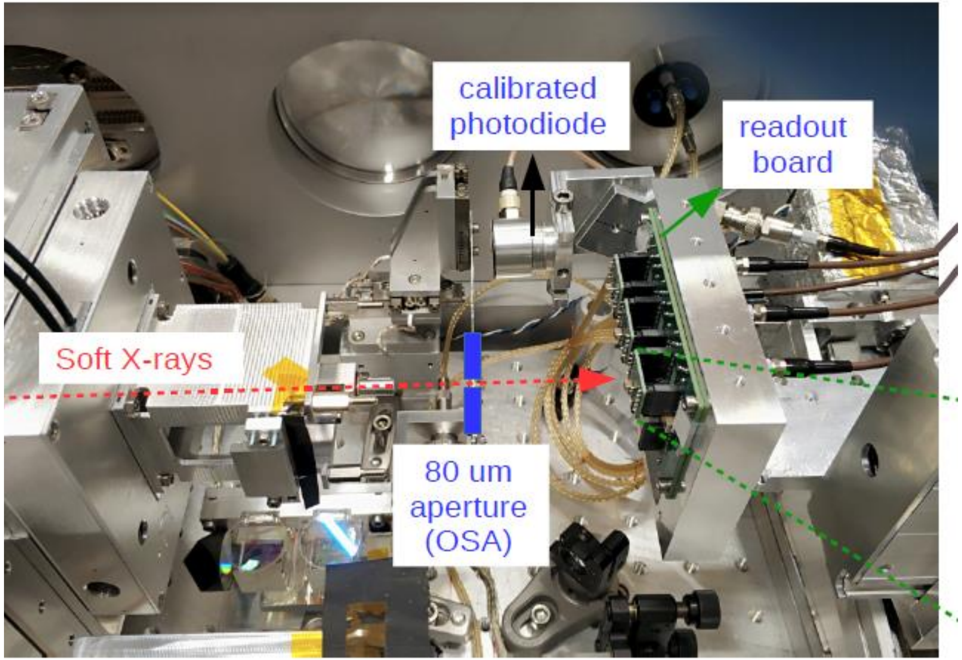

*Courtesy of M. Carulla

Pixelated iLGAD setup

- Illumination with a Fresnel zone plate +OSA
- Peltier system to cool the sensor to -40°C

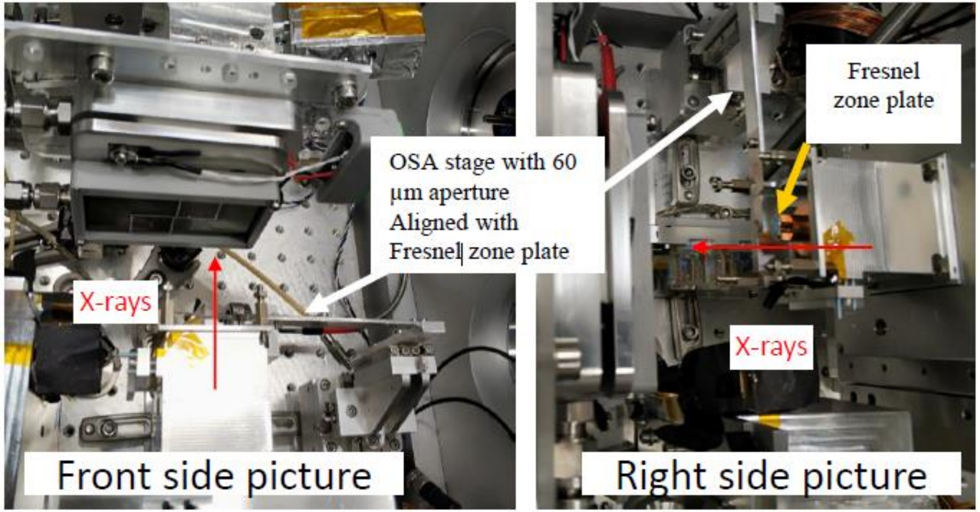

*Courtesy of M. Carulla

QE vs E_{ph} for all process splits

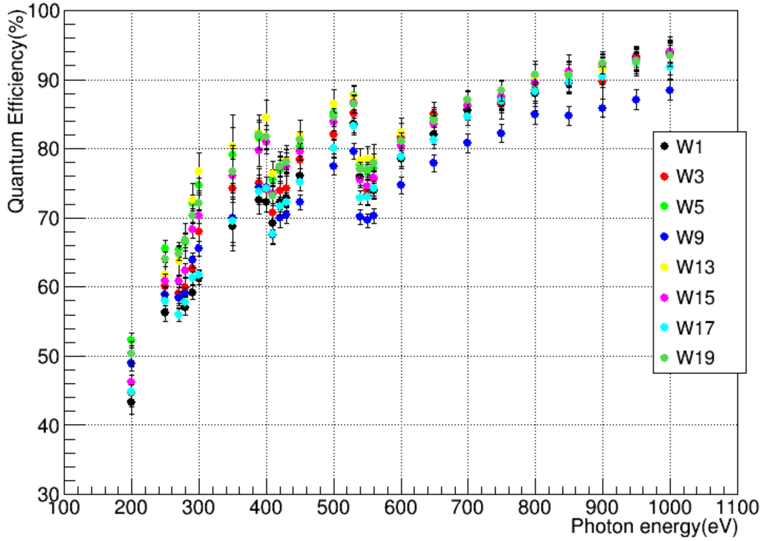

$$QE = \frac{I_{ph}}{I_{ph\ c}} QE_c$$

PAUL SCHERRER INSTITUT

Higher harmonics contamination

$$\eta_{measured}(E_{ph}) = \frac{I_L(E_{ph}) + I_H(E_{ph})}{I_{Lc}(E_{ph}) + I_{Hc}(E_{ph})}\eta_c(E_{ph})$$

$$\eta_{measured}(E_{ph}) = \frac{\eta_L \eta_{Lc}}{\eta_{Lc} + n\left(\frac{\Phi_H}{\Phi_L}\right)\eta_{Hc}} + \frac{\eta_H \eta_{Lc}}{\eta_{Hc} + \frac{1}{n}\left(\frac{\Phi_L}{\Phi_H}\right)\eta_{Lc}}$$

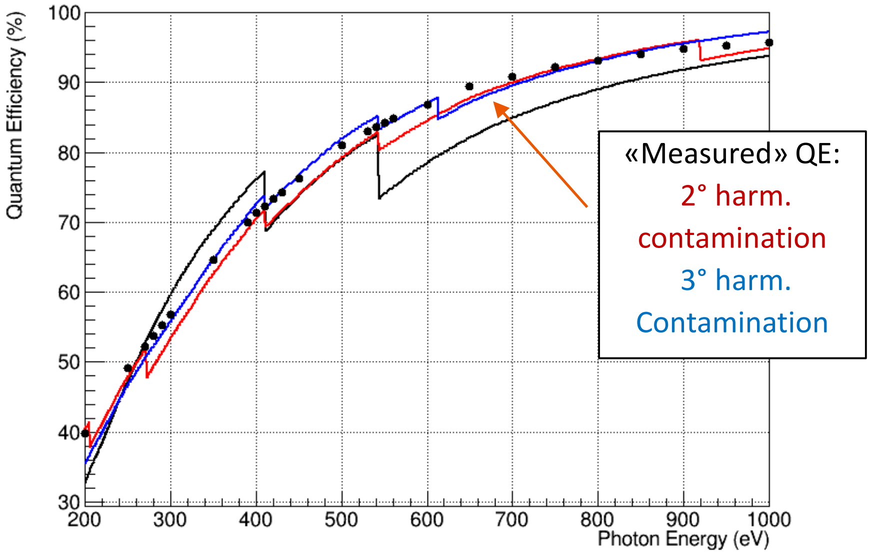

Higher harmonic contamination determines an **underestimation of $\mathrm{QE}(E_{ph})$** if the calibrated photodiode has a quantum efficiency $\mathrm{QE0}(E_{ph}) < \mathrm{QE}(E_{ph})$. This is the case **at low E_{ph}.**

Gain vs E_{ph} for all process splits

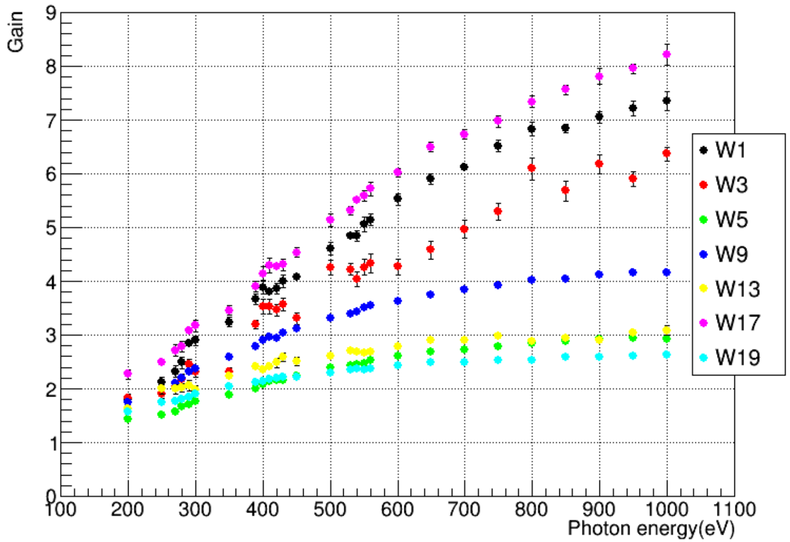

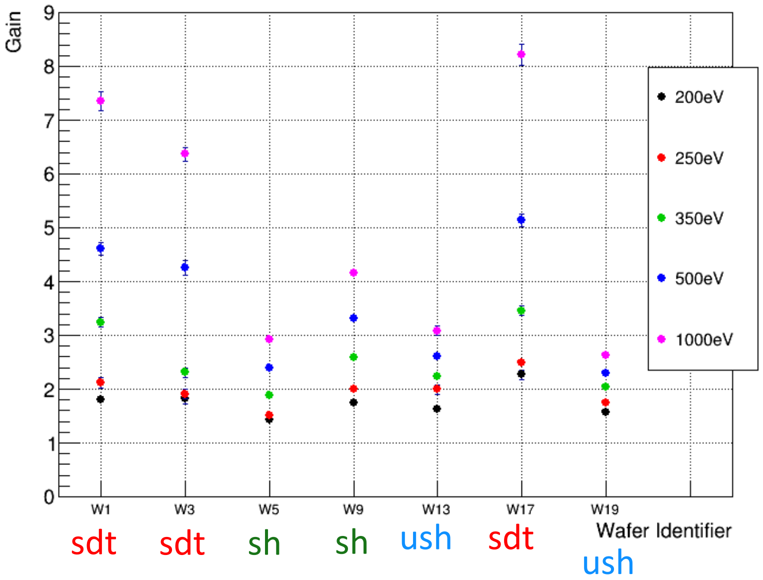

$$G_{iAaLGAD} = \frac{\frac{I_{ph\ iLGAD}}{I_{ph\ c1}}}{\frac{I_{ph\ pin}}{I_{ph\ c2}}}$$

iLGAD diodes: gain vs E_{ph} & **linear** model for $M(z)$

Gain vs E_{ph} - iLGADs with standard GL (W17) and shallow GL (W9)

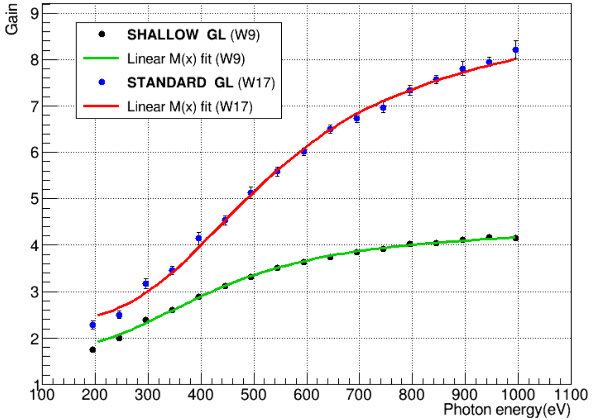

Gain expression (assuming CCE =1) :

$$g_{iLGAD}(E_{ph}) \sim \int_0^W \mu(E_{ph}) e^{-\mu(E_{ph})\cdot z} \cdot M(z)dz$$

With **linear model M(z) in GL**

$$M(z) = \begin{cases} M_h \;\; if\; z \leq t_1 \\ linear \;\; t_1 \leq z \leq t_2 \\ M_e \;\; if\; t_2 \leq z \end{cases}$$

From fit of Linear M(z) model:

Standard GL:	**Shallow GL:**
$\boldsymbol{M_e = 8.9} \pm 0.1$	$\boldsymbol{M_e = 4.4} \pm 0.02$
$\boldsymbol{M_h = 2.3} \pm 0.1$	$\boldsymbol{M_h = 1.78} \pm 0.05$
$t_1 = 112nm\ (fixed)$	$t_1 = 107nm\ (fixed)$
$\boldsymbol{t_2 = 690nm} \pm 40nm$	$\boldsymbol{t_2 = 330nm} \pm 40nm$

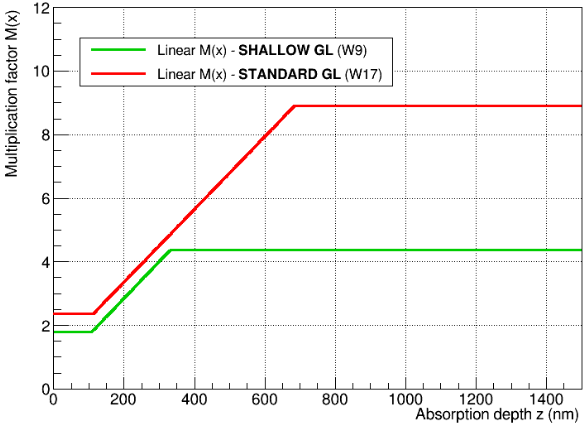

iLGAD diodes: gain vs E_{ph} & **exponential** model for $M(z)$

Gain vs E_{ph} - iLGADs with standard GL (W17) and shallow GL (W9)

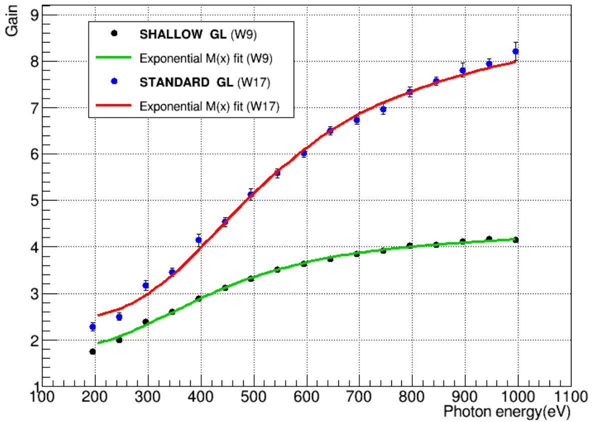

Gain expression (assuming CCE =1) :

$$g_{iLGAD}(E_{ph}) \sim \int_0^W \mu(E_{ph}) e^{-\mu(E_{ph})\cdot z} \cdot M(z)dz$$

With **exponential model M(z) in GL**

$$M(z) = \begin{cases} M_h & if\ z \leq t_1 \\ exponential & t_1 \leq z \leq t_2 \\ M_e & if\ t_2 \leq z \end{cases}$$

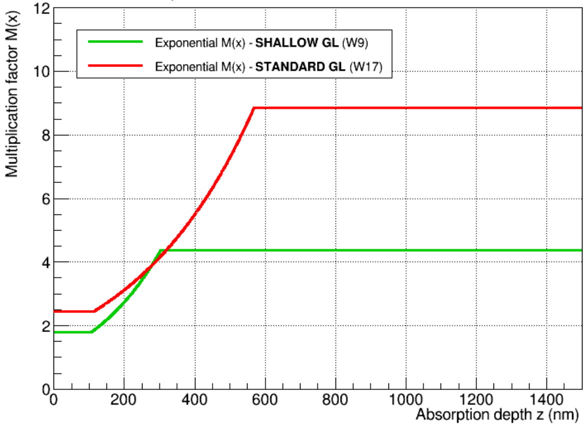

From fit of exponential M(z) model:

Standard GL:	**Shallow GL:**
$\boldsymbol{M_e} = \mathbf{8.8} \pm 0.1$	$\boldsymbol{M_e} = \mathbf{4.4} \pm 0.02$
$\boldsymbol{M_h} = \mathbf{2.44} \pm 0.08$	$\boldsymbol{M_h} = \mathbf{1.80} \pm 0.06$
$t_1 = 112nm\ (fixed)$	$t_1 = 107nm\ (fixed)$
$\boldsymbol{t_2} = \mathbf{570nm} \pm 30nm$	$\boldsymbol{t_2} = \mathbf{303nm} \pm 20nm$

Gain vs beam intensity at 350eV and 700eV

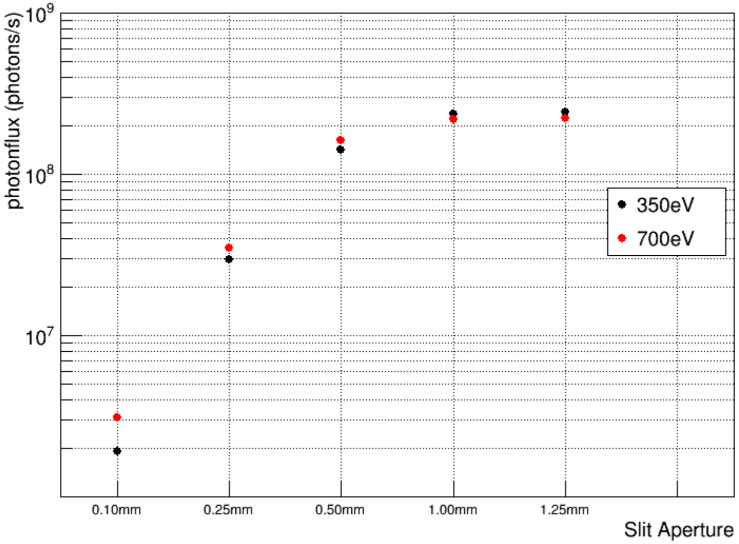

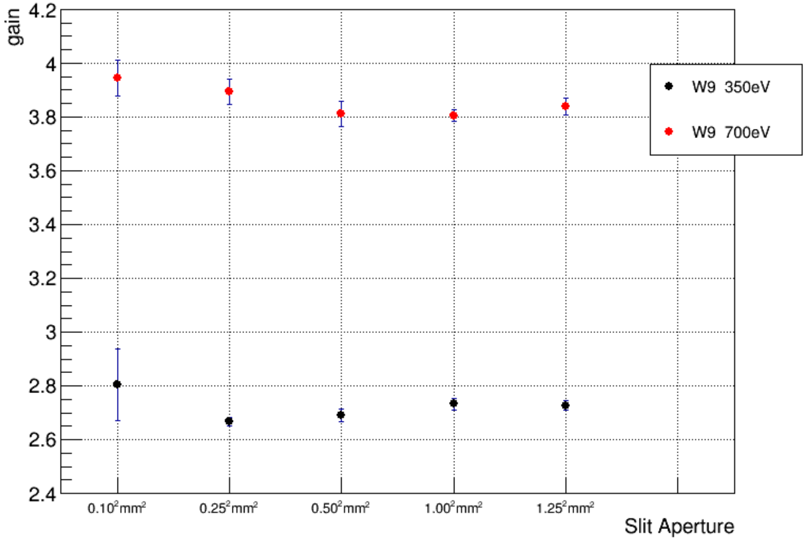

$$\frac{dNph}{dt} = \frac{I_{ph} * 3.6eV}{e * QE * E_{ph}}$$

Un-calibrated spectra

$$E_{ph} = 500eV$$

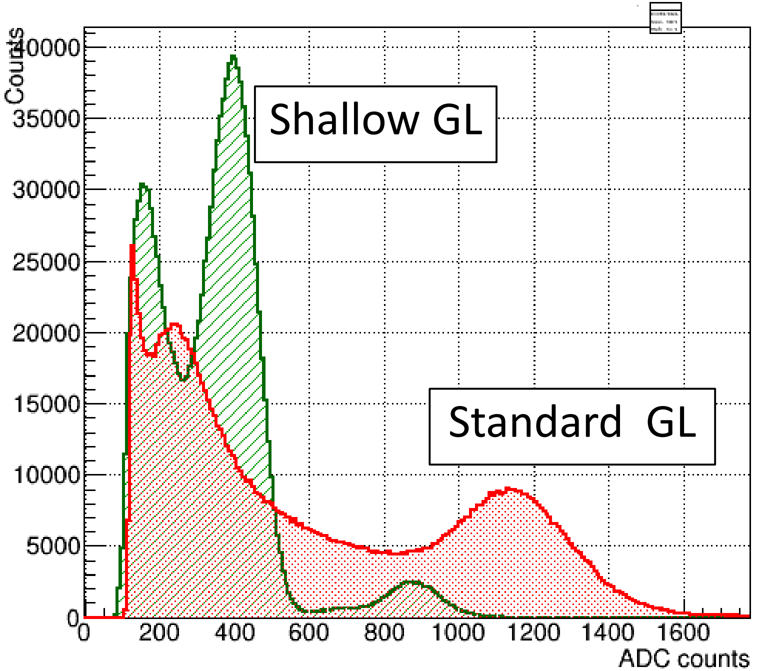

Scaling of the ratio Mh/Me for temperature change wrt +20°C: different models comparison

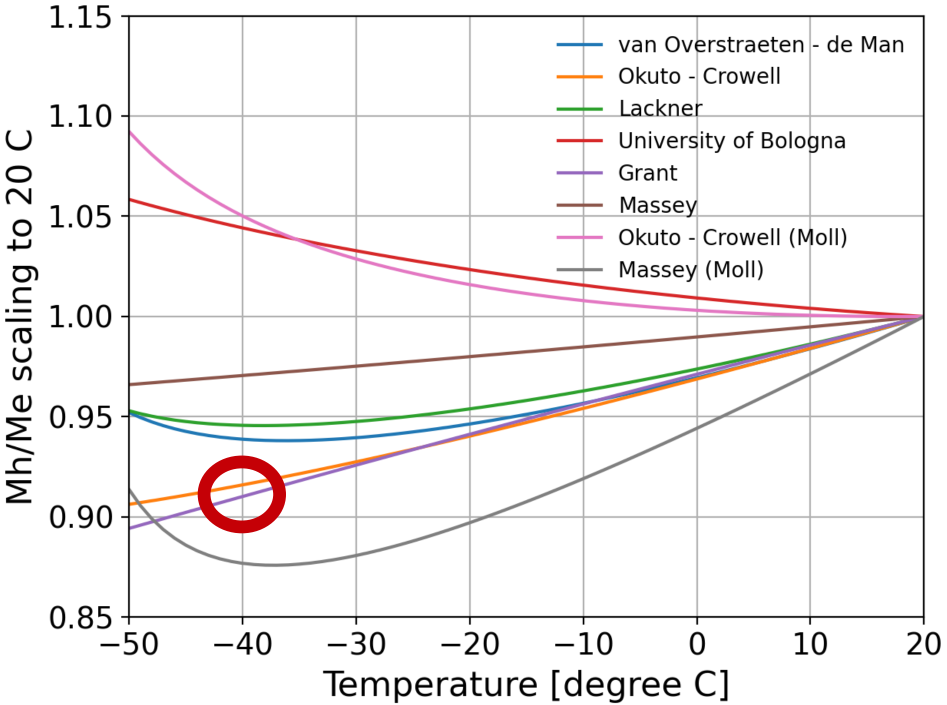

Validation of the mobility model for simulation

- The model is a combination of :
- Arora model (for the description of the doping dependence)

- Jacoboni and Selberherr models (for the T dependence)

- Extended Canali model (for the E-field dependence)

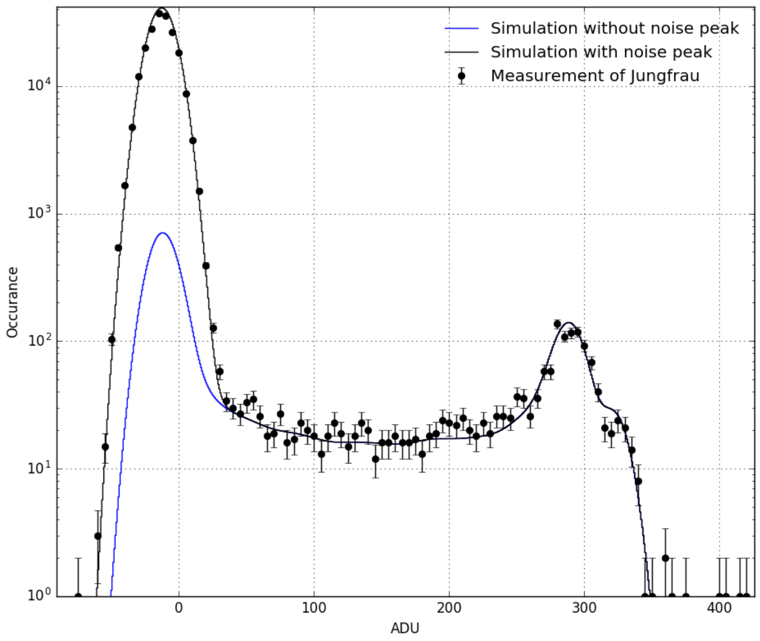

Chi2 minimization wrt shot noise scaling parameter σ_1